INRIA

INSTITUT NATIONAL DE RECHERCHE EN INFORMATIQUE ET EN AUTOMATIQUE

CONSERVATION CORRECTION BY DUAL LEVEL SET

Anne-Cécile Lesage, Alain Dervieux, Damien Guégan

N° 7089

November 2009

Thème NUM

ISSN 0249-6399 ISRN INRIA/RR--7089--FR+ENG

INRIA
SOPHIA ANTIPOLIS

CONSERVATION CORRECTION BY DUAL LEVEL SET

Anne-Cécile Lesage*, Alain Dervieux†, Damien Guégan‡

Thème NUM — Systèmes numériques
Projet Pumas

Rapport de recherche n° 7089 — November 2009 — 29 pages

Abstract: When applied to the simulation of bi-fluid incompressible flow, the level set method does not ensure mass conservation of each fluid. Now this needs to be enforced. In this paper, we propose a complementary local mass conservation based on a weak formulation of the advection of the interface characteristic function. We first apply our method to the advection of a discontinuous concentration. Secondly, we couple our method with incompressible two-phase flow simulation and validate it on test cases where one fluid separates in disconnected parts (motion of two separated liquid volumes, water column falling on an obstacle).

Key-words: Computational Fluid Dynamics, finite volume, unstructured meshes, level set, interfaces

* Barcelona Supercomputing Center BSC-CNS C/ Gran Capitán 2, 2a. Planta 08034 Barcelona - Spain
† INRIA, 2004 Route des Lucioles, BP. 93, 06902 Sophia-Antipolis, France
‡ LEMMA, 06410 Biot, France

Unité de recherche INRIA Sophia Antipolis
2004, route des Lucioles, BP 93, 06902 Sophia Antipolis Cedex (France)
Téléphone : +33 4 92 38 77 77 — Télécopie : +33 4 92 38 77 65

CORRECTION DE CONSERVATION PAR DUALE LEVEL SET

Résumé : La méthode level set appliquée à un écoulement bi-fluide incompressible ne conserve pas le volume de chaque phase. Or il est utile de le conserver. Dans ce papier, nous proposons une approche complémentaire baseé sur une formulation faible de l'advectionde la fonction caractéristique. La méthode est d'abord appliquée à la simple advection d'une fonction caractéristique. Puis la nousvelle méthode est couplèe à un modèle bi-fluide incompressible appliqué à des écoulements avec des composantes séparées d'une des phases (mouvement dans un double réservoir et chute de colonne d'eau sur un obstacle).

Mots-clés : Mécanique des Fluides Numérique,volumes finis, maillages non-structurés, ligne de niveau, interfaces

1 INTRODUCTION

Prediction of interface motion in two-phase incompressible flow simulation is of important interest for applied research and engineering. This subject involves a difficult approximation problem. The interface involves macro-scales for example when capillarity is modelled on the basis of a smooth interface woth curvature, and micro scales (breaking,...).

Standard Lagrangian Methods present difficulties to simulate break-up events, *Particle Lagrangian Methods* seem not easy to model boudary layers and capillarity, *Eulerian Methods* present difficulties to advect the interface with a good accuracy. In the subset of *Eulerian Methods*, The Volume-of-Fluid (VOF) method [1] brings an elegant method for keeping a non-diffused interface and the conservation of each phase mass. But it is rather dependant of the initial finite-volume basic approximation, which limits its extension to other numerical technologies. The Level Set Method (LS in the sequel) developped in the 80's by Osher and Sethian ([2],[3]) uses the zero level contour of a smooth function ϕ to locate the interface. The LS variable ϕ is advected with flow velocity:

$$\phi_t + \mathbf{V}\nabla\phi \ = \ 0 \ .$$

In contrast to VOF methods, LS has a continuous statement and can be easily adapted to a larger family of discretization methods, paving the way to high-order approximations.

However, mass conservation is not naturally satisfied by LS. This is correlated to two particular steps of LS, the advection of LS and the re-distancing of it. Let us consider the case of an incompressible flow with two immiscible fluids. The volume occupied by each fluid should remain constant. The satisfaction of this property by an Eulerian method is a rather complex issue. Two different contexts should be kept in mind. When mesh is enough finer than interface's smaller detail, conservation is perfectly satisfied by methods like VOF and satisfied up to a small error by non-conservative methods like LS.
When an evolution of the interface becomes smaller than mesh size, conservative methods like VOF may produce unphysical artefacts which in some cases are lost for the phase component from which it separated. Non-conservative methods like non-conservative LS may behave even worse, loosing a rather important mass amount. In the case of complex interface evolution, this event is frequent and then standing by high-order resolution for mass conservation is not reasonable.

These remarks have motivated the development of conservative or quasi-conservative LS methods.

Globally mass-conserving methods refer to corrections of the LS ensuring the exact conservation of total mass. An interesting improvement consists in correcting the interface location proportionally to the normal velocity length, see [9]. They carry some improvement, see for example [14], but this kind of improvement does not provide a complete answer to the question risen here, of having a more *local conservation*. For example, flow with disconnected components of a same phase should conserve constant mass for each component.
Let us also mention the attempts to reduce mass loss arising from a particular stage of LS algorithm, for example the redistancing stage, see [13]. We focus now on the conservation issue after the advection step. As remarked in many works, advection can be conservative for the LS variable ϕ,

$$\phi_t + div(\mathbf{V}\phi) \ = \ 0$$

but this property does not implies mass conservation of phases. In [5], a method is proposed for using a parametrisation of interface that will be stiffer than the LS, but still smooth in order to

improve the mass conservation at advection step.
In most other approaches, a finite-volume method applied to a characteristic function of a phase is explicitly introduced. In [6], both LS and VOF are combined and produce an hybrid scheme that is a kind of improvement of both methods. The discrete dependant variable for interface is also a synthesis of LS ans VOF representations. The assembly of a VOF method is rather complex and instead, a more simple finite-volume method can be applied to a characteristic function derived from the LS field. This is the idea proposed in [4]. With this kind of approach, the difficult step is to derive a level set solution from the finite-volume predictor. In [4], this is performed by a Newton pointwise relaxation.

From these works it appears that starting from an accurate LS, getting an exact conservation is paid by a return to a less accurate finite-volume scheme in order to get a FV solution to be tranformed back into LS representation.

The present work is motivated by the quest of a corrector to an accurate LS without passing by a finite-volume scheme, but saving the LS accuracy when conservation is closely satisfied by the LS solution and improving its accuracy in the other case.

We restrict to the incompressible multifluid model. Let us examine the particular case of a unique choice of approximation, viz. vertex centered on unstructured meshes, applied at the same time to LS, to velocity components and to pressure. The main interest of this choice is its simplicity. However, the velocity approximation does not satisfy a (discrete or not) zero divergence relation.

In this paper, we first recall the principle of Level Set representation for the advection of a characteristic function. Then we examine the issue of mass conservation in case where the advecting velocity is of zero divergence. We present a new local mass conservation enforcement method which produces an approximative local conservation. Our method uses a local conservation condition based on a weak formulation of the advection equation of the characteristic function $H(\phi)$ of one phase.

$$\int \psi H(\phi)_t + \phi \mathbf{V} \psi \; dv \; = \; 0 \; , \forall \; \psi$$

Where the test function ψ lies in a smooth approximation space. Since the unknown variable remains the LS function, while smoothness issue is transfered to the test function, the standpoint is *dual* to the classical Level Set formulation. In the present paper, this formulation is applied to a standard P1 finite-element framework. Evaluation of the new scheme is done with two interface advection test cases (Zalesak test case, vortex flow test case). The combination of the local mass conservation method with a projection method for Navier-Stokes is then presented. It is applied to incompressible two phase flow test cases (motion of two separated liquid volumes, water column falling on an obstacle).

2 ADVECTION OF A CHARACTERISTIC FUNCTION

2.1 Basic Level Set scheme

The advection of an interface can, under some smoothness assumption concerning the subdomains limited by it, be written with the characteristic function χ of one phase (to fix the ideas, the "liquid" phase):

$$\chi = 1 \quad \textit{liquid phase}$$
$$\chi = 0 \quad \textit{gaz phase}$$

Starting from an initial location χ_0, it is advected with a *divergence-free* velocity field $\tilde{\mathbf{U}}$ that is assumed to be given in this section.

$$\frac{\partial \chi}{\partial t} \; + \; \nabla\cdot(\tilde{\mathbf{U}}\chi) \; = \; 0 \quad \chi(x,0) = \chi_0(x). \tag{1}$$

The formal accuracy of the numerical advection of a step function like χ is limited to first order unless the numerical scheme cleverly exploits the fact that χ takes only two different values.

Let H be the step function such that $H(x) = 1$ if $x > 0$ and $H(x) = 0$ elsewhere. The Level Set method introduced by Osher et Sethian ([10]) relies on two smoother functions, $\phi_0(x)$ such that $H(\phi_0(x)) = \chi(x,0)$ and $\phi(x,t)$ such that:

$$\frac{\partial \phi}{\partial t} \; + \; \nabla\cdot(\tilde{\mathbf{U}}\phi) \; = \; 0 \quad \phi(x,0) = \phi_0(x). \tag{2}$$

We take $\phi \; < \; 0$ in the gas region and $\phi \; > \; 0$ in the liquid region. The interface is the zero level set of ϕ:

$$\Gamma \; = \; \{\mathbf{x} \mid \phi(\mathbf{x},t) = 0\} \tag{3}$$

It is useful now to introduce a time discretization for the LS advection. Let $\bar{\phi}^n$ be the discretized in time LS function. We apply a tree-stage time advancing. A variational formulation with a test function ψ writes:

$$\begin{aligned}
\int_\Omega \psi_i \bar{\phi}^{n+\frac{1}{3}} dv &= \int_\Omega \psi_i \bar{\phi}^n dv + \frac{\Delta t}{3}\int_{\partial\Omega} \psi_i \bar{\phi}^n \tilde{\mathbf{U}}\cdot\mathbf{n} d\Gamma - \frac{\Delta t}{3}\int \phi^n \tilde{\mathbf{U}}\cdot\nabla\psi_i dv \\
\int_\Omega \bar{\psi}_i \bar{\phi}^{n+\frac{1}{2}} dv &= \int_\Omega \psi_i \bar{\phi}^n dv + \frac{\Delta t}{2}\int_{\partial\Omega} \psi_i \bar{\phi}^{n+\frac{1}{3}} \tilde{\mathbf{U}}\cdot\mathbf{n} d\Gamma - \frac{\Delta t}{3}\int \bar{\phi}^{n+\frac{1}{3}} \tilde{\mathbf{U}}\cdot\nabla\psi_i dv \\
\int_\Omega \psi_i \bar{\phi}^{n+1} dv &= \int_\Omega \psi_i \bar{\phi}^n dv + \Delta t\int_{\partial\Omega} \psi_i \bar{\phi}^{n+\frac{1}{2}} \tilde{\mathbf{U}}\cdot\mathbf{n} d\Gamma - \Delta t\int \bar{\phi}^{n+\frac{1}{2}} \tilde{\mathbf{U}}\cdot\nabla\psi_i dv
\end{aligned} \tag{4}$$

With this formulation, the inflow boundary value is directly introduced in place by specifying $\bar{\phi}$. Initial condition $\bar{\phi}^0$ can be defined as the signed-distance to the initial interface but the advected field $\bar{\phi}$ will not stay in general a distance to its zero level set. An usual practice is refered as "redistancing" and consists of resetting function $\bar{\phi}$ as the distance to interface $\bar{\phi} \; = \; \pm\, d(\Gamma)$. This is done by various means, in particular by solving a Hamilton-Jacobi equation ([11],[12], or by direct geometrical construction.

2.2 Global mass conservation

An important property of incompressible two-phase flow is the volume conservation of each phase which expresses in terms of $\chi = H(\phi)$:

$$\chi_t + \nabla.(\chi\tilde{\mathbf{U}}) = 0 \;\Rightarrow\; \int \chi_t dx = V_{liquid,t} \tag{5}$$

where $V_{liquid,t} = \frac{d}{dt}V_{liquid}$ is the (given) rate of liquid carried through the domain boundaries. For simplicity, we assume this rate is zero. One of the important drawbacks of the level set method is the loss of conservation of this formulation because of the use of ϕ. It is possible to conserve ϕ by solving $\phi_t + \nabla.(\phi\tilde{\mathbf{U}}) = 0$ but this does not imply the conservation of each phase.

In [14], Smolianski proposes a global mass conservation which corrects at each time step ϕ_h^{n+1} into $\overline{\phi}_h^{n+1}$. The idea is to add a small uniform perturbation C^{n+1} to ϕ^{n+1} in each point of the domain to ensure conservation of the constant volume of the liquid phase, the initial value of which writes $V^0_{liquid} = \int H(\bar{\phi}^0)dv$. This method uses the property that starting with a signed distance function ($\nabla\phi^{n+1} = 1$) and adding a constant correction C_ϕ will not change the signed distance function property. The function

$$\Phi(C) \;=\; \int H(\bar{\phi}_h^{n+1} + C)dv$$

is strictly monotone with a derivative bounded from zero, since it expresses in terms of the level set contour length (2D case):

$$\frac{d\Phi}{dC}(C) \;\approx\; \text{length}(\{x, \bar{\phi}_h^{n+1}(x) + C = 0\}) \tag{6}$$

Then, in the modified version that we use in [7], we exactly solve the following statement of mass conservation:

$$\begin{aligned} &\text{Find } C^{n+1} \text{ such that } \int H(\bar{\phi}_h^{n+1} + C^{n+1})dv = V^0_{liquid} \\ &\overline{\phi}_h^{n+1} \;=\; \bar{\phi}_h^{n+1} + C^{n+1}. \end{aligned} \tag{7}$$

The solution C^{n+1} is determined by a Newton (*regula falsi*) method. As far as $H(\phi_h)$ is an higher order accurate approximation of χ, the error in $\int |H(\phi_h) - \chi|dv$ is of higher order and the global volume correction step will not degrade the accuracy.
This method brings some improvement for two-phase incompressible test cases when each fluid is forming an unique volume. An interesting improvement is proposed in [9]. It consists of making the amount of mass taken or added (according to the global spurious lack or supplement) proportional to the absolute value of the normal velocity of the interface. Global mass algorithms are not completely satifactory. Typically, in the case where one fluid is disconnected in separated volumes, the global mass conservation does not ensure the conservation of each volume.

2.3 Local mass conservation

As already mentioned, a local discrete mass conservation is not satisfied by the LS method under study. It is due to several reasons:

(i) The discrete velocity field is not divergence free,

(ii) The advection of ϕ in general does not satisfy the conservation of $H(\phi)$,

(iii) Advection of details of the interface that are too small for the mesh size will result in numerically clipping these details and will not satisfy conservation,

(iv) Redistancing does not in general satisfy conservation.

Point (iii) desserves some comments: moving for example a small isolated bubble around a vertex A, with size less than cell size, to a position B located $\Delta x/2$ farther will result in the wrong approximation the bubble motion. Indeed, the new bubble exact position cannot be represented by the LS method inside an element. Either the bubble is not moved correctly or it disappears. From these remarks, it results that strict local conservation cannot easily be applied with our options. Therefore, our standpoint is to derive local correctors for improving the local conservation. These correctors will be used in the same way as the previous global corrector.

In this section, we shall present an analysis allowing us to build a local correction of the Level Set function. We are looking for a non constant corrector $C^{n+1}(\mathbf{x})$. Our method is based on a enforcement of the incompressiblility constraint on the nodes located in the interface neighbourhood.

Let us assume that the velocity field is divergence free, the interface motion can be described by both of these two conservation laws (with $\chi = H(\phi)$).

$$\phi_t + \nabla \cdot (\tilde{\mathbf{U}}\phi) = 0 \tag{8}$$
$$\chi_t + \nabla \cdot (\tilde{\mathbf{U}}\chi) = 0 \tag{9}$$

In the continuous case, (8) implies (9) but this does not extend in general in the discrete case.

We would like to recover (9) without deteriorating the advection accuracy of ϕ. Indeed, we do not want to replace a non-conservative advection of high order accuracy by a conservative advection but of lower order.

2.3.1 Dual formulation

To correct the mass conservation of ϕ in the neighbourhood of the interface, we are searching to solve the following *Dual Level Set* equation on the elements intersected by the interface :

$$\forall \psi_i \in P_1, \int_\Omega \psi_i (H(\phi))_t dv = \int_{\partial\Omega} \psi_i H(\phi)\tilde{\mathbf{U}} \cdot \mathbf{n} d\Gamma - \int H(\phi)\tilde{\mathbf{U}} \cdot \nabla\psi_i dv \tag{10}$$

The forward-Euler time-dicretization of (10) gives

$$\begin{aligned} \forall \psi_i \in P_1, \int_\Omega \psi_i H(\phi^{n+1}) dv &= \int_\Omega \psi_i H(\phi^n) dv + \Delta t \Big(\int_{\partial\Omega} \psi_i H(\phi)\tilde{\mathbf{U}} \cdot \mathbf{n} d\Gamma \Big) \\ &- \Delta t \Big(\int H(\phi)\tilde{\mathbf{U}} \cdot \nabla\psi_i dv \Big) . \end{aligned} \tag{11}$$

We verify that it implies the mass conservation of both phases by summing for all i:

$$\int_\Omega H(\phi^{n+1}) dv - \int_\Omega H(\phi^n) dv = \Delta t \Big(\int_{\partial\Omega} H(\phi)\tilde{\mathbf{U}} \cdot \mathbf{n} d\Gamma - \int H(\phi)\tilde{\mathbf{U}} \cdot \nabla 1 \; dv \Big) = 0 . \tag{12}$$

In practice, we use a multi-step Runge-Kutta 3 time dicretization with a MUSCL scheme of second-order accuracy [7] in order to compute ϕ^{n+1}. We deduce $\phi^{n+\frac{1}{2}}$ of the second step of 3-stage

Runge-Kutta scheme. Thus we obtain an accurate approximation of (10).

$$\begin{aligned} \forall \psi_i \in P_1, \int_\Omega \psi_i H(\phi^{n+1}) dv &= \int_\Omega \psi_i H(\phi^n) dv + \Delta t \Big(\int_{\partial\Omega} \psi_i H(\phi^{n+\frac{1}{2}}) \tilde{\mathbf{U}} \cdot \mathbf{n} d\Gamma \Big) \\ &- \Delta t \Big(\int H(\phi^{n+\frac{1}{2}}) \tilde{\mathbf{U}} \cdot \nabla \psi_i dv \Big) \end{aligned} \tag{13}$$

Although the number of unkowns (values of ϕ in each node) is apparently the same as the number of equations (number of basis function ψ_i), the system (13) is not necessarily well set, since this system does not depend on values of ϕ at nodes far from interface. In particular, it does not always admit a solution, for example when the interface presents too small details for the mesh (component of one phase smaller than one cell). On the other end for sufficiently smooth discrete interfaces, the system (13) can help us to build an efficient local volume correction.

In the case where the region where $H(\phi^{n+\frac{1}{2}}) = 0$ contains the entire support of ψ_i for some i, the system reduces to

$$\int_\Omega \psi_i H(\phi^{n+1}) dv = \int_\Omega \psi_i H(\phi^n) dv$$

which implies that a candidate solution would would satisfy $H(\phi^{n+1}) = H(\phi^n)$ on $Supp\psi_i$.

In the case where the region where $H(\phi^{n+\frac{1}{2}}) = 1$ contains the support of ψ_i, the system reduces to

$$\begin{aligned} \int_\Omega \psi_i H(\phi^{n+1}) dv &= \int_\Omega \psi_i H(\phi^n) dv + \Delta t \Big(\int_{\partial\Omega} \psi_i \tilde{\mathbf{U}} \cdot \mathbf{n} d\Gamma + \int \tilde{\mathbf{U}} \cdot \nabla \psi_i dv \Big) \\ &= \int_\Omega \psi_i H(\phi^n) dv + \Delta t \int \psi_i \; div \tilde{\mathbf{U}} \; dv \; . \end{aligned} \tag{14}$$

Assuming that the advection velocity is divergence-free, this case reduces to the previous one. In both cases, the equation expresses that the sign of ϕ is constant but does not specify more than this, which illustrates -if necessary- that the problem is ill-posed in terms of ϕ.

For the sequel of this analysis, we shall make an assumption a little more restrictive than a CFL-like one. We observe that function $H(\phi^{n+1})$ (resp.$H(\phi^{n+\frac{1}{2}}), H(\phi^n)$ is not strictly 0 or 1 only on a subset I_{n+1}, (resp.$I_{n+\frac{1}{2}}, I_n$) of the set of supports of ψ_i:

$$I_{n+1} = \bigcup_j Supp\psi_j$$

where the union is taken for all test functions ψ_j such that $\nabla H(\phi^{n+1})$ is not identically zero on $Supp\psi_j$. We consider in our analysis the simplified case where:

$$I_{n+1} = I_{n+\frac{1}{2}} = I_n$$

2.3.2 Lax-Wendroff accuracy analysis

We assume that we have a sequence of functions $\hat{\phi}_h$, each $\hat{\phi}_h$ verifying on the mesh τ_h the following equation :

$$\forall \psi_i \in P_1, \int_\Omega \psi_i (H(\hat{\phi}_h))_t dv = \int_{\partial\Omega} \psi_i H(\hat{\phi}_h) \tilde{\mathbf{U}} \cdot \mathbf{n} d\Gamma - \int H(\hat{\phi}_h) \tilde{\mathbf{U}} \cdot \nabla \psi_i dv + h^k R_i^h \tag{15}$$

where R_i^h is uniformly bounded independently of h and of node i.

We give now some heuristic elements of error analysis between function $\hat{\phi}_h$ and the continuous solution ϕ of system (10). The system having a weak solution, we can use the Lax-Wendroff principle for convergence of weak solutions. We write Problem (10) as follows :

$$\forall\ \psi\ \in\ \mathcal{D}(\bar{\Omega}\times]0,T[), \Big(\ \chi_t + \nabla\cdot(\tilde{\mathbf{U}}\chi)\ ,\ \psi\Big)_{\bar{\Omega}\times]0,T[} = 0 \tag{16}$$

Let Π_h be an interpolation operator in V_h, we write the discrete problem (15) as follows:

$$\forall\ \psi\ \in\ \mathcal{D}(\bar{\Omega}\times]0,T[), \Big(\ \chi_{h,t} + \nabla_h\cdot(\tilde{\mathbf{U}}\chi_h)\ ,\ \Pi_h\psi\Big)_{\bar{\Omega}\times]0,T[} = h^k R^h(\psi) \tag{17}$$

where $R^h(\psi)$ is uniformly bounded independently of h.
We transpose the derivation operator on the test function ψ.
In the continuous case :

$$\Big(\chi\ ,\ -\psi_t - \tilde{\mathbf{U}}\cdot\nabla\psi\Big)_{\bar{\Omega}\times]0,T[} = 0\ . \tag{18}$$

In the discrete case :

$$\Big(\chi_h\ ,\ -\Pi_h\psi_t - \tilde{\mathbf{U}}\cdot\nabla_h^*\cdot\Pi_h\psi\Big)_{\bar{\Omega}\times]0,T[} = h^k R^h(\psi)\ . \tag{19}$$

By difference, we obtain :

$$\begin{aligned}\Big(\chi-\chi_h\ ,\ -\psi_t - \tilde{\mathbf{U}}\cdot\nabla\psi\Big)_{\bar{\Omega}\times]0,T[} = \\ \Big(\chi_h\ , -\psi_t - \tilde{\mathbf{U}}\cdot\nabla\psi + \Pi_h\psi_t + \tilde{\mathbf{U}}\cdot\nabla_h^*\cdot\Pi_h\psi\Big)_{\bar{\Omega}\times]0,T[} \\ -h^k R^h(\psi)\ .\end{aligned} \tag{20}$$

The second member can be analysed with the following estimations :

$$||\chi_h||_{L^\infty} = 1, \tag{21}$$

$$||\psi_t - \Pi_h\psi_t||_{L^p} = (O)(h^2), \tag{22}$$

completed by the assumption that the spatial derivation operator is second order accurate in the following sense :

$$||\nabla\psi - \nabla_h^*\cdot\Pi_h\psi||_{L^p} = (O)(h^2). \tag{23}$$

The following error estimate comes out :

$$\Big(\chi-\chi_h\ ,\ -\psi_t - \tilde{\mathbf{U}}\cdot\nabla\psi\Big)_{\bar{\Omega}\times]0,T[} = h^k|R^h(\psi)| + (O)(h^2)\ . \tag{24}$$

Thus this approach seems likely to conserve the second-order accuracy.

Since a solution does not always exists, a stability analysis, that indeed would be useful, seems out of reach at the moment. Although needing iteration for being advanced, the scheme is of explicit type and is probably subject to a CFL condition. The last step is also of central difference type but we have not met in experiments a clear need for adding dissipation.

2.3.3 Definition of the conservative corrector

We rewrite the previous problem as follows:

$$\begin{aligned}
\text{Find } \phi^{n+1} \quad & \text{so that } \Psi_i(\phi^{n+1}) = 0 \ \ \forall\, i, \text{ with} \\
\Psi_i(\phi) &= \int_\Omega \psi_i H(\phi) dv - b_i \\
b_i &= \int_\Omega \psi_i H(\phi^n) dv \\
&+ \Delta t(-\int_{\partial\Omega} \psi_i H(\phi^{n+\frac{1}{2}}) \tilde{\mathbf{U}} \cdot \mathbf{n} d\Gamma) + \int_\Omega H(\phi^{n+\frac{1}{2}}) \tilde{\mathbf{U}} \cdot \nabla \psi_i dv)
\end{aligned} \tag{25}$$

We observe that a diagonal evaluation of the derivative of Ψ can be done as follows:

$$\frac{\partial \Psi_i}{\partial \phi_i} \ \approx \ \int \psi_i dx \ dx \ .$$

This can be used to re-dimensionalize the dual LS residual:

$$\hat{\Psi}_i(\phi) \ = \ \Psi_i(\phi) / \int \psi_i dx \ dx \quad ; \quad \hat{\Psi}(\phi) = \sum \hat{\Psi}_i(\phi) \psi_i .$$

We propose a first simplified corrector by applying a non-uniform correction to the Level Set function ϕ:

$$\begin{aligned}
&\text{Let } \phi^{n+1} \text{obtained from primal LS} \\
&\text{Find } C^{n+1} \text{such that:} \\
&\int \phi_i^{n+1} \ + \ C^{n+1} \hat{\Psi}_i(\phi^{n+1}) \ dx \ = \ V, \\
\text{Put } \tilde{\phi}_i^{n+1} \ &= \ \phi_i^{n+1} \ + \ C^{n+1} \hat{\Psi}_i(\phi^{n+1}) \quad \forall\, i
\end{aligned}$$

However, since the corrector field is of arbitrary sign, we cannot ensure the monotony of the new functional:

$$\int \phi_i^{n+1} \ + \ C^{n+1} \hat{\Psi}_i(\phi^{n+1}) \ dx \ - \ V \ .$$

It is only locally monotone when its derivative is not zero. This means that only a sufficiently small C^{n+1} can be applied in order to decrease the mass loss. In the non-frequent case of a zero derivative, we can make the derivative non-zero by adding to the corrector a small uniform perturbation. In

practice, this algorithm brings an interesting improvement with respect to the global correction, as will be illustrated in the sequel by numerical experiments

In a more sophisticated iteration, we try to minimise the residual of the dual LS system by a Picard fixed point:

0. $\tilde{\phi}^{(0)} = \tilde{\phi}^{n+1}$
1. Compute: $F(\eta) = ||\hat{\Psi}_i(\phi^{(\alpha)} + \eta\Psi_i(\phi^{(\alpha)}))||$ for: $\eta = \varepsilon, \eta = -\varepsilon$
If $Min(F(\varepsilon), F(-\varepsilon), F(0)) = F(0)$ then stop
$\varepsilon' = ArgMin(F(\varepsilon), F(-\varepsilon))$
$\phi^{(\alpha+1)} = \phi^{(\alpha)} + \eta\Psi_i(\phi^{(\alpha)})$
where η is chosen with same sign as ε' and such that:
$\Psi_i(\phi^{(\alpha+1)}) < \Psi_i(\phi^{(\alpha)})$
2. Go to 1

The choice of η can be performed efficiently by relaxing from the Newton step for F which writes:

$$\begin{aligned} F' &= (F(\varepsilon') - F(0))/\varepsilon' \\ \eta_0 &= 0 - (F')^{-1}F(0) \\ \phi^{(\alpha+1)} &= \phi^{(\alpha)} + \eta_0\Psi_i(\phi^{(\alpha)}) \end{aligned} \tag{26}$$

If F depends linearly on η, the choice $\eta = \eta_0$ converges in one step. In general it does not guarantee convergence and we search the smallest non-negative integer n for which $\eta = \eta_0/2^n$ satisfies $\Psi_i(\phi^{(\alpha+1)}) < \Psi_i(\phi^{(\alpha)})$.

Remark: In contrast to the standard Level Set formulation, the Dual LS system defines the function ϕ only near the interface. It can be combined with a re-distancing process for defining the other degrees of freedom of ϕ.

In the following section, we will compare the performance of the new local corrector with the global corrector on two interface advection test cases (Zalesak disk).

3 INTERFACE ADVECTION NUMERICAL EXAMPLES

3.1 Rotation of Zalesak's disk

Consider the rigid body rotation of Zalesak's disk in a constant vorticity velocity field [15]. The initial interface is slotted circle centered at $(50., 75.)$ with a radius of 15., a width of 5., and a slot length of 25. Velocity is given by $u = (\pi/314)(50 - y)$ and $v = (\pi/314)(x - 50)$ so that the disk completes one revolution every 628 time units. The Level Set funtion is initialised like the signed distance function to the Zalesak's disk. We compute one revolution of the Zalesak's disk on three

embedded meshes 101×101, 201×201, 401×401. We define the relative error of the L_1 norm as $\frac{\|H(\phi_h)-H(\phi_{exact})\|_{L_1}}{\|H(\phi_{exact})\|_{L_1}}$.

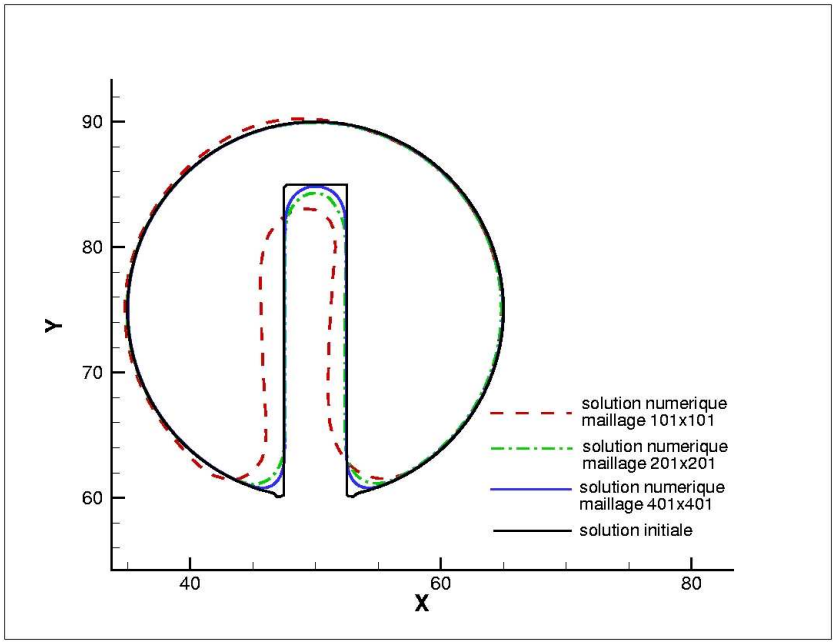

Figure 1: *Rotation of Zalesak's disk. Mesh Convergence results after one revolution. Global mass conservation algorithm*

We compute the numerical convergence order as follows :

$$n = \frac{ln||H(\phi_h) - H(\phi^{exact})||_{L_1}^{finemesh} - ln||H(\phi_h) - H(\phi^{exact})||_{L_1}^{coarsemesh}}{ln(\delta x)^{finemesh} - ln(\delta x)^{coarsemesh}} \tag{27}$$

Figure 1 illustrates the mesh convergence results after one full rotation with the global mass corrector. Figure 2 illustrates the mesh convergence results with the local mass corrector. Table 1 and 2 give the results on relative error L_1 on the full rotation on the three meshes. It permits to compute the convergence order on $H(\phi)$ with equation (27). We observe a clear improvement of the relative error L_1 with the local mass corrector. On the 401×401 nodes, the error with the local corrector is three time less important as with the global corrector.

3.2 Single vortex

While Zalesak's disk is a good indicator of diffusion error in an interface-capturing method, it does not test the ability of an Eulerian scheme to accurately resolve thin filaments on the scale of the mesh which can occur in strectching and tearing flows for example in the turbulent case. A flow which exhibits interface streching is the "vortex-in-a-box" problem introduced by Bell *et al.* [16]. Figure 3 shows the nonconstant vorticity velocity field centered in the box with the largest velocity

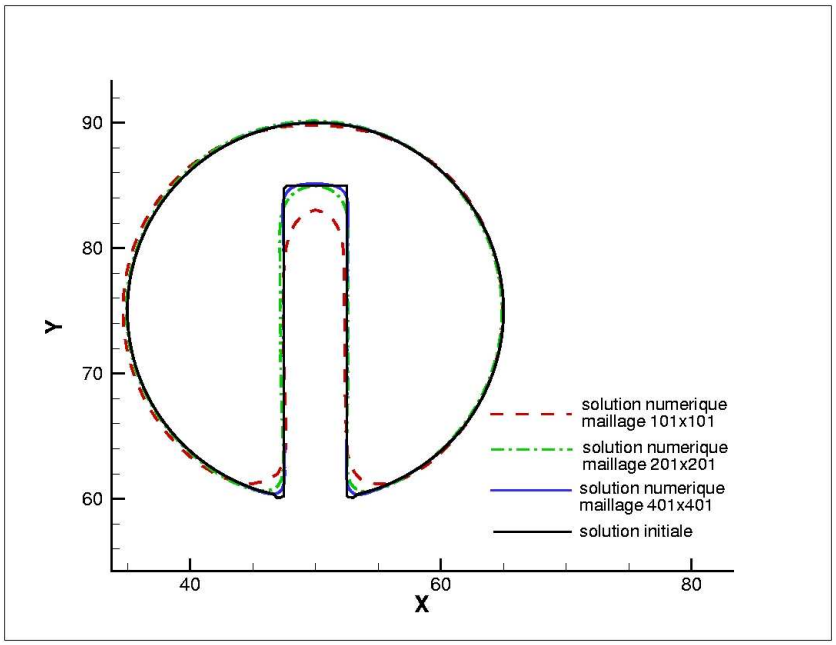

Figure 2: *Rotation of Zalesak's disk. Mesh Convergence results after one revolution. Local mass conservation algorithm*

Number of nodes	Relative error L_1	Convection Order on $H(\phi)$
101x101	0.158	-
201x201	0.0418	1.94
401x401	0.0203	1.04

Table 1: Rotation of Zalesak's disk : relative error L_1 between the exact function $H(\phi_{exact})$ and $H(\phi_h)$ after one revolution with the **global mass corrector algorithm**. Convergence order results.

Number of nodes	Relative error L_1	Convection Order on $H(\phi)$
101x101	0.0674	-
201x201	0.0148	2.18
401x401	0.007	1.08

Table 2: Rotation of Zalesak's disk : relative error L_1 between the exact function $H(\phi_{exact})$ and $H(\phi_h)$ after one revolution with the **local mass corrector algorithm**. Convergence order results.

located half way to the walls of the domain. The velocity field is defined by the stream function

$$\Psi = \frac{1}{\pi} sin^2(\pi x) sin^2(\pi y).$$

A unit computational domain is used with a circle of radius 0.15 placed at $(0.5, 0.75)$. The resulting velocity field streches out the circle into a very long, thin fluid element which progressively wraps itself toward the center of the box. Figure 4 shows the comparison of the level set solution for the vortex flow at $t = 1s$ with the global corrector and with the local corrector algorithm. We can observe that the result on the coarse mesh 101×101 nodes with the local corrector is far better than the one with the global corrector. We even observe if we compare with the higly accurate result provided by Enright *et al.* [17] with their particle Level Set Method that the local corrector on 101×101 nodes mesh presents even better accuracy than the converged solution on 401×401 nodes mesh using the global corrector. Figures 6 and 8 compare our level set solution with the local corrector on the 201×201 nodes mesh with the solution of Enright *et al.* [17] with the highly accurate particle level set method Figure 7 and 9 on 128×128 at $t = 3$ and $t = 5$. Enright *et al.* [17] use particle advected in a lagrangian way to correct the zero level set contour, they have artificially very fine mesh. We are not as accurate as these authors, but comparing with the fineness of the lagrangian nodes they use, it seems in fact that our discretization is much coarser.

This test case proves as for the previous Zalesak's disk test the improvement achieved with the new local corrector. In the next section, we will couple our local corrector with Navier-Stokes model of two phase instationary incompressible flows.

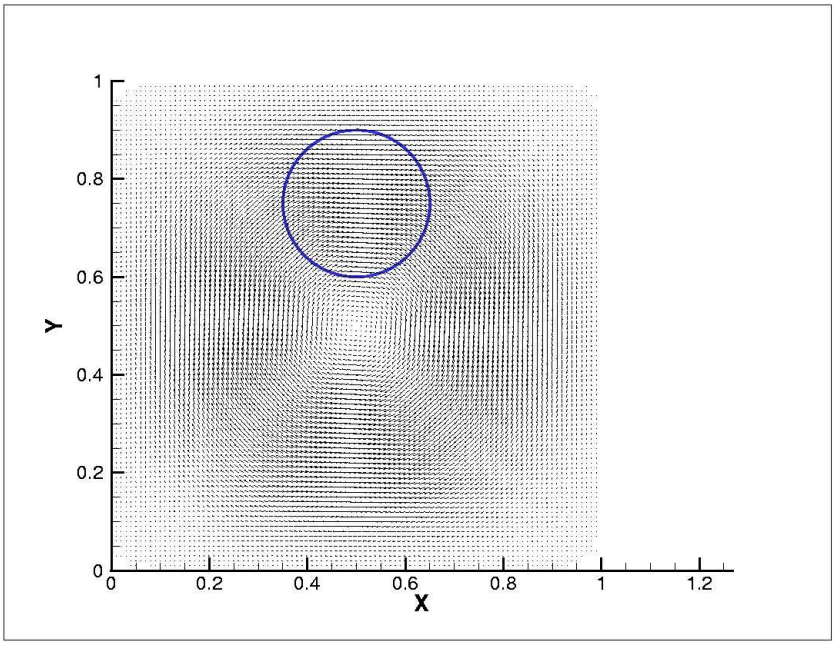

Figure 3: *Initial data and velocity field for the vortex flow.*

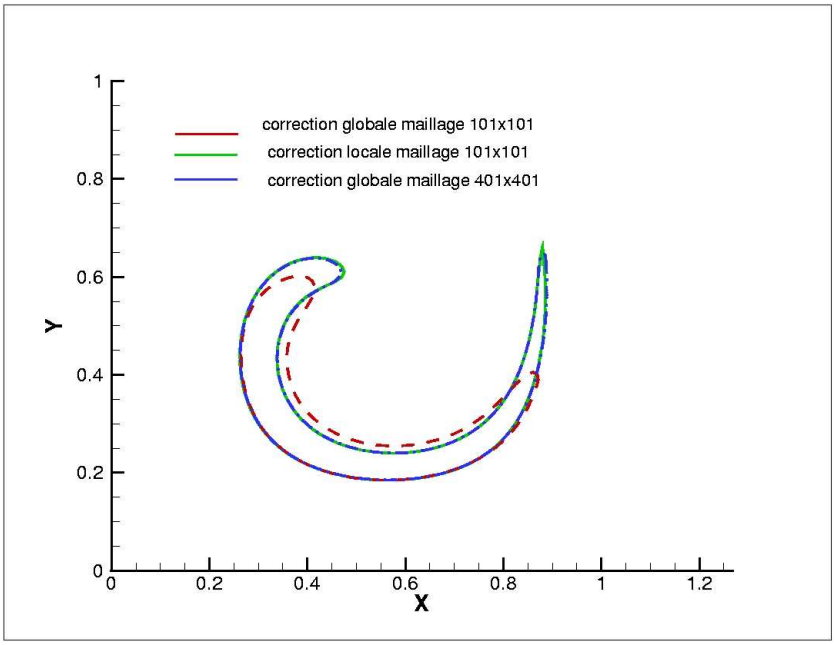

Figure 4: *Comparison of the level set solution for the vortex flow at* $t = 1s$ *with the global corrector and with the local corrector algorithm. Red level set solution with global corrector on* 101×101 *nodes mesh. Green level set solution with local corrector on* 101×101 *nodes mesh. Blue level set solution with global corrector on* 401×401 *nodes mesh.*

4 LEVEL SET METHOD FOR TWO-PHASE INCOMPRESSIBLE FLOW

4.1 Differential model

Let us consider the solution of the model of two incompressible immiscible fluids moving in a closed vessel Ω with no-slip wall condition, under the influence of gravity but without interface tension. It writes for the fluid velocity $\mathbf{U}$, the pressure p and the density ρ as follows:

$$\begin{aligned} \rho\frac{\partial \mathbf{U}}{\partial t} + \rho\nabla.(\mathbf{U}\times\mathbf{U}) - \nabla.(2\nu(\rho)\nabla\mathbf{U}) + \nabla p - \rho\mathbf{g} &= 0 \ \text{ in } \Omega\ , \\ \partial_t\rho + \nabla.(\rho\mathbf{U}) = 0 \qquad \rho = \rho_l \text{ or } \rho_g \ &\text{ in } \Omega\ , \\ \nabla.\mathbf{U} = 0 \ &\text{ in } \Omega\ , \\ \mathbf{U} = 0 \ &\text{ on } \partial\Omega\ . \end{aligned} \tag{28}$$

In this formulation, the density takes in Ω only two real positive values ρ_l and ρ_g in two subdomains separated by an interface smooth enough for allowing to consider its normal:

$$\mathbf{n}\delta(\rho) = \frac{1}{\rho_l - \rho_g}\nabla\rho\ . \tag{29}$$

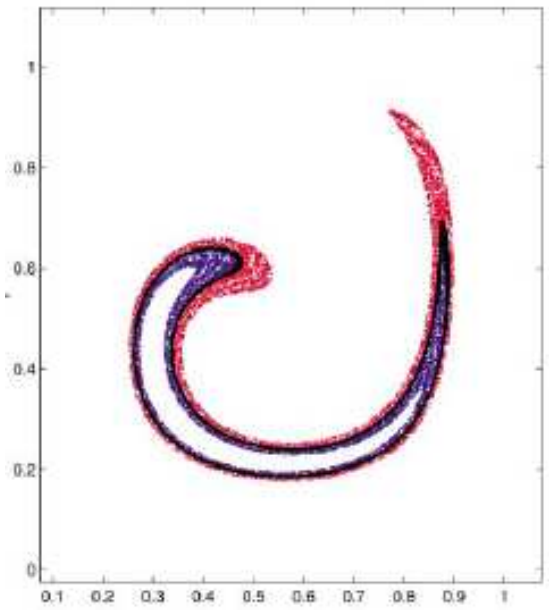

Figure 5: *Particle Level Set Method solution (black) for the vortex flow at* $t = 1$ *cf Enright et al.[17].*

To fix the ideas, ρ_l in the liquid and ρ_g in the gas. Further, $\delta(\rho)$ denotes the Dirac delta function on the interface, $\mathbf{g}$ the gravity volumic force, and $\nu(\rho)$ the viscosity.

The interface advection is performed by the level set method with the characteristic function χ of liquid phase.

$$\phi_t + div(\mathbf{V}\phi) = 0 \;\; ; \;\; \chi = H(\phi) \tag{30}$$

with an advect exactly equal to material velocity, i.e. $\mathbf{V} = \mathbf{U}$. The density and the viscosity are constant in each fluid, we can write

$$\begin{aligned} \rho(\phi) &= \rho_g + (\rho_g - \rho_l)\, H(\phi) \\ \nu(\phi) &= \nu_g + (\nu_g - \nu_l)\, H(\phi). \end{aligned} \tag{31}$$

Then the previous governing equations for the fluid velocity $\mathbf{U}$ and the pressure p along with boundary conditions can be written as:

$$\rho(\phi)\frac{D\mathbf{U}}{Dt} = -\nabla p + \nabla.(2\nu(\phi)D) + \rho(\phi)\mathbf{g} \tag{32}$$

4.1.1 Approximation

Let us now choose a numerical method for advancing the incompressible velocity. We consider for simplicity a first-order time-accurate projection method for the P1-P1 space discretisation as in [7]. Several important improvement for stability ad accuracy have been proposed, see for example the recent paper [**?**]. Let Ω_h be a discretisation of Ω_h covered by a triangulation $\mathcal{T}_h$. Discrete domain

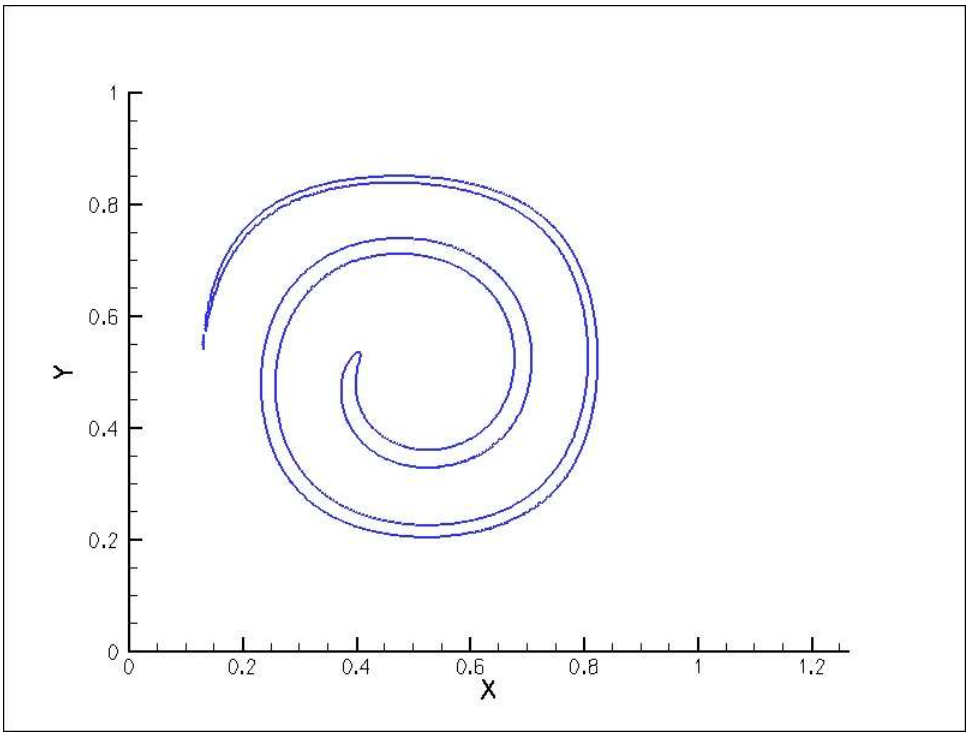

Figure 6: *Level set solution for the vortex flow at* $t = 3s$ *with local corrector algorithm on* 201×201 *nodes mesh.*

Ω_h is assumed to be identical to Ω. For simplicity of notations, index h of space discretisation is also omitted for other symbols. We introduce the usual P1 finite-element space:

- $V = \{\psi \in \mathcal{C}^0(\bar{\Omega}), \psi|_T$ is affine $\forall T \in \mathcal{T}\}$

V is spanned by the set of basis functions ψ_i for any i, where ϕ_i is equal 1 on vertex i and zero on other vertices.

- $\mathbf{V} = V^d$, where $d = 2$ is the space dimension.

the space of functions that are constant by element is denoted:

-$H = \{v \in L^2(\Omega), v|_T$ is constant $\forall T \in \mathcal{T}\}$

- $\mathbf{H} = H^d$.

Projection in $\mathbf{H}$*:* for all $U = (u, v)$ in $(L^2(\Omega))^2$, we denote: $\mathcal{P}_0 u$ the function of H such that for any element T of $\mathcal{T}$, $\mathcal{P}_0 u|_T = \int_T u dxdy / \int_T dxdy$ and we denote also $\mathcal{P}_0 U = (\mathcal{P}_0 u, \mathcal{P}_0 v)$.

Projection in $\mathbf{V}$*:* for all $U = (u, v)$ in $\mathbf{H}$, we denote: $\mathcal{P}u$ the function of V such that for any i, vertex of $\mathcal{T}$, $\mathcal{P}u|_i = \int u\psi_i dxdy / \int \psi_i dxdy$ and we denote also $\mathcal{P}U = (\mathcal{P}u, \mathcal{P}v)$.

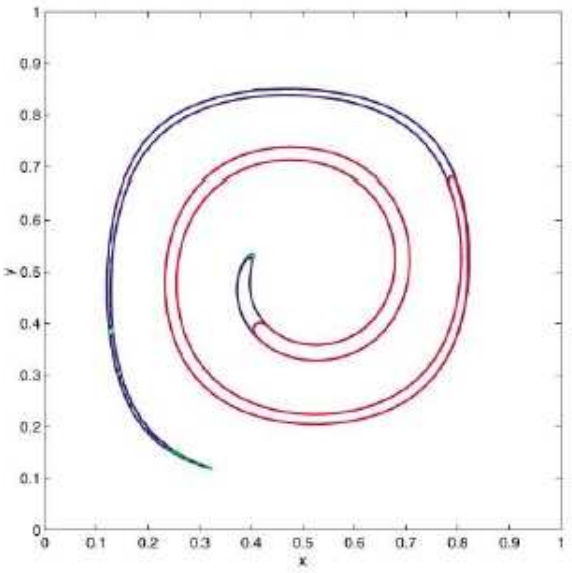

Figure 7: *Particle Level Set Method solution (blue) for the vortex flow at $t = 3$ cf Enright et al.[17].*

Mass lumping: we call cell area the following mass-lumped coefficient:

$$area(i) \;=\; \sum_j \int_\Omega \psi_i \psi_j dv \;.$$

The discretised multi-fluid variables are:

$$\mathbf{U} \;=\; \sum_i \mathbf{U}_i \psi_i \;\;,\;\; p \;=\; \sum_i p_i \psi_i \;\;,\;\; \phi \;=\; \sum_i \phi_i \psi_i \;.$$

The global algorithm for advancing them in time writes:

Stage 1: (Prediction) Compute an explicit predictor for moment:

$$\bar{\mathbf{U}}_i \;=\; \mathbf{U}_i^n - \Delta t \; area(i)^{-1} \int_\Omega \psi_i \left(\nabla.(\mathbf{U} \times \mathbf{U}) \;-\; \frac{1}{\rho} \nabla.(2\nu(\rho) \nabla \mathbf{U}) \;-\; \mathbf{g} \right) dv \;. \tag{33}$$

Stage 2: (Projection) Solve in V the elliptic system:

$$\int \frac{1}{\rho} \nabla p . \nabla \psi dx dy \;=\; \frac{1}{\Delta t} \int \nabla \psi . \bar{\mathbf{U}} dx dy \tag{34}$$

and put:

$$\mathbf{U}^{n+1} = \bar{\mathbf{U}} + \Delta t \; \mathcal{P} \left(\frac{1}{\rho} \nabla p \right) \;\;,\;\; \mathbf{U}^{n+1} = 0 \;\; \text{on } \partial\Omega. \tag{35}$$

Stage 3: (LS advection) Advect the ϕ function with V from time level n to time level $n+1$, for example with the three-stage scheme (11). In practise, we stabilize this central-differenced scheme

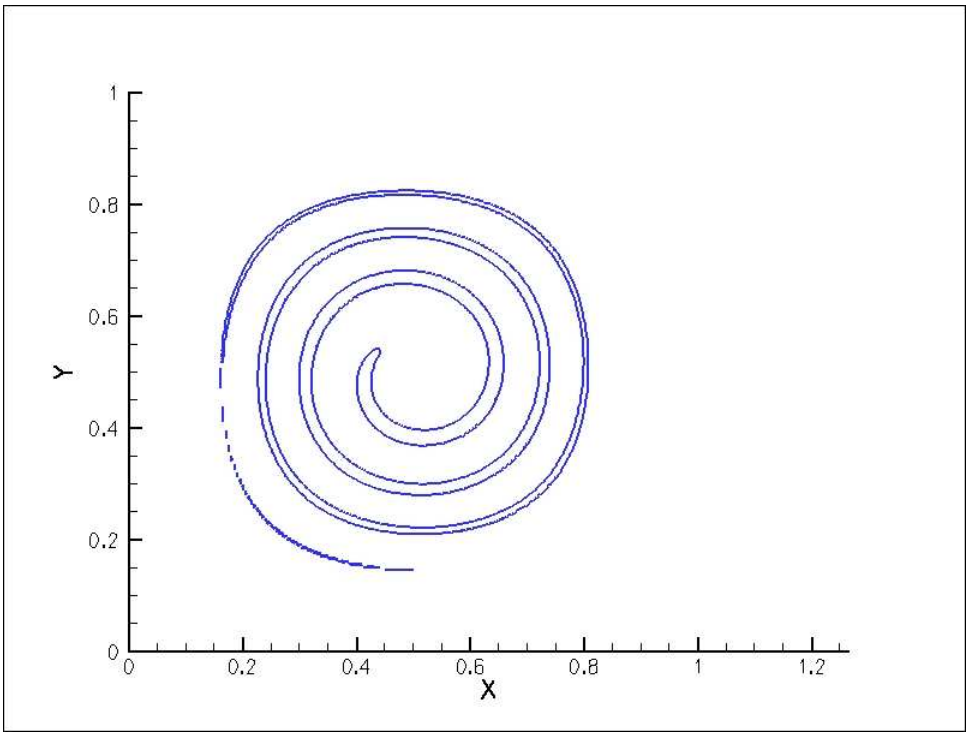

Figure 8: *Level set solution for the vortex flow at* $t = 5s$ *with local corrector algorithm on* 201×201 *nodes mesh.*

with a MUSCL cell-wise reconstruction.

Stage 4: (Redistancing) Replace the advected $\bar{\phi}^{n+1}$ by a reinitialised or redistanced $\tilde{\phi}^{n+1} =$ signed distance to $\{\bar{\phi}^{n+1} = 0\}$,,

Stage 5: (Conservation) Replace the re-initialised $\tilde{\phi}^{n+1}$ by a ϕ^{n+1} enjoying a conservation property.

4.2 Enforcement of the incompressibility constraint

To correct ϕ through a conservative advection of χ, it is necessary to determine a velocity field $\tilde{\mathbf{U}}$ satisfying the discrete incompressiblity constraint identified as:

$$\int_{\Omega} \psi_i div\tilde{\mathbf{U}}\, dv \quad = \quad 0 \quad , \forall\, i \tag{36}$$

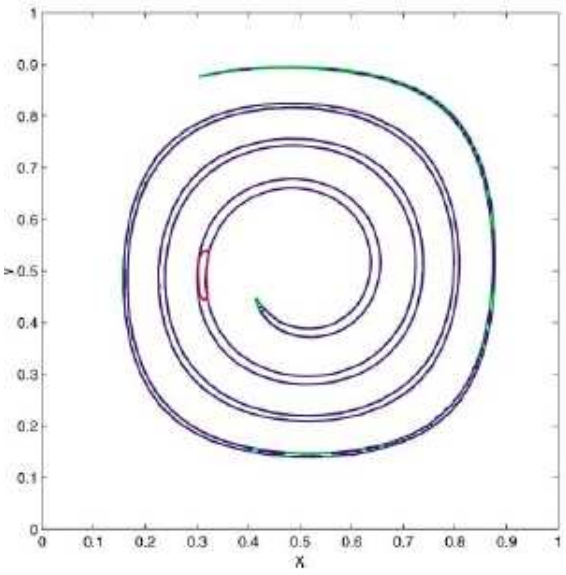

Figure 9: *Particle Level Set Method solution (blue) for the vortex flow at $t = 5$ cf Enright et al.[17].*

With the proposed projection method, this constraint is not satisfied by the solution $\mathbf{U}^{n+1}$ of (35). Let us introduce the following approximation of velocity:

$$\tilde{\mathbf{U}} = \mathcal{P}_0 \bar{\mathbf{U}} + \frac{1}{\rho} \nabla p \tag{37}$$

where p is the solution of (34).

Lemma: *(i) The P_0 velocity field $\tilde{\mathbf{U}}$ defined in (37) satisfies:*

$$\int_\Omega \tilde{\mathbf{U}} \nabla \psi_i \, dv = 0 \quad \forall \; i \tag{38}$$

(ii) By advecting the χ function with the velocity field $\tilde{\mathbf{U}}$, mass conservation far from the interface is verified in the following sense :

$$\forall \psi_i \text{ tel que } H(\phi)|_{supp\psi_i} \quad \equiv \quad 1, \int_\Omega \psi_i (H(\phi))_t dv = 0. \tag{39}$$

Indeed, the discrete conservation satisfied by $\tilde{\mathbf{U}}$ is imposed by the projection step in each node i. For the nodes internal to the mesh, we have

$$\int \nabla \psi_i \cdot \tilde{\mathbf{U}} = 0. \tag{40}$$

where ψ_i is the basis function P_1 at node i.

We can write a spatial semi-discretization of (9) under the following variational form.

$$\forall \psi \in P_1,\ \iint \psi(H(\phi))_t \ + \ \iint \psi \nabla \cdot (\mathbf{U} H(\phi)) = 0. \tag{41}$$

Using an integration by part, we get

$$\int_\Omega \psi(H(\phi))_t dv = \int_{\partial\Omega} \psi H(\phi)\mathbf{U}\cdot\mathbf{n} d\Gamma - \int H(\phi)\mathbf{U}\cdot\nabla\psi dv \tag{42}$$

The equation (42) becomes for ψ_i:

$$\int_\Omega \psi_i(H(\phi))_t dv = -\int \mathbf{U}\cdot\nabla\psi_i dv\ , \tag{43}$$

and if we use of velocity field $\tilde{\mathbf{U}}$ with the propriety (40), we obtain (39). □

Thus the use of $\tilde{\mathbf{U}}$ allows us to control the approximation errors on the velocity divregence far from the interface.

Then this velocity field is introduced in all advection formula for ϕ and in particular in (11).

5 TWO PHASE INCOMPRESSIBLE FLOW NUMERICAL EXAMPLES

5.1 Liquid oscillation in two separated tanks

As first test case of two phase incompressible flow, we compute the oscillation of a water volume under gravity. The tank of 1 meter long is separated in two parts by a thick wall. We assume the fluids are non viscid and the density ratio of $1:1000$. The air-water interface shape is initialized as a stable horizontal interface in the right side tank and as a curve in the left side tank (cf figure 10). As the motion occurs in the left side tankand the interface is immobile in the right side tank, the whole mass errors is done in the left part. By construction, the global mass conservation algorithm corrects the mass lost in the left side by spreading out this correction in both sides. This incapacity of the global mass conservation to distinguish equilibrium area and the correction of two disconnected part of one phase is an important weakness expecially for industrial applications. Figure 11 shows the interface position at $t = 1s$ for both mass correction algorithm (global corrector cf section 3, local corrector cf section 4) on two embedded meshes. When we apply the local correction algorithm, the interface level remains very closed to the exact position. For the fine mesh, the global corrector (in green) has changed the interface position at right and this deviation is twice larger in the case of the coarse mesh. Figure 12 represents time evolution of mass loss in the tank left side for the two options global mass corrector and local mass corrector on two embedded mesh. The error with the local corrector is at the maximum of 0.1%. This very small error is due to loss produced by redistanciation which are corrected in the globally and to the numerical errors of the local corrector algorithm. On the contrary for the global correction algorithm, the error is rather important $(4-8\%)$.

On this test case, the local corrector proved to solve the important weaknesses of the global corrector.

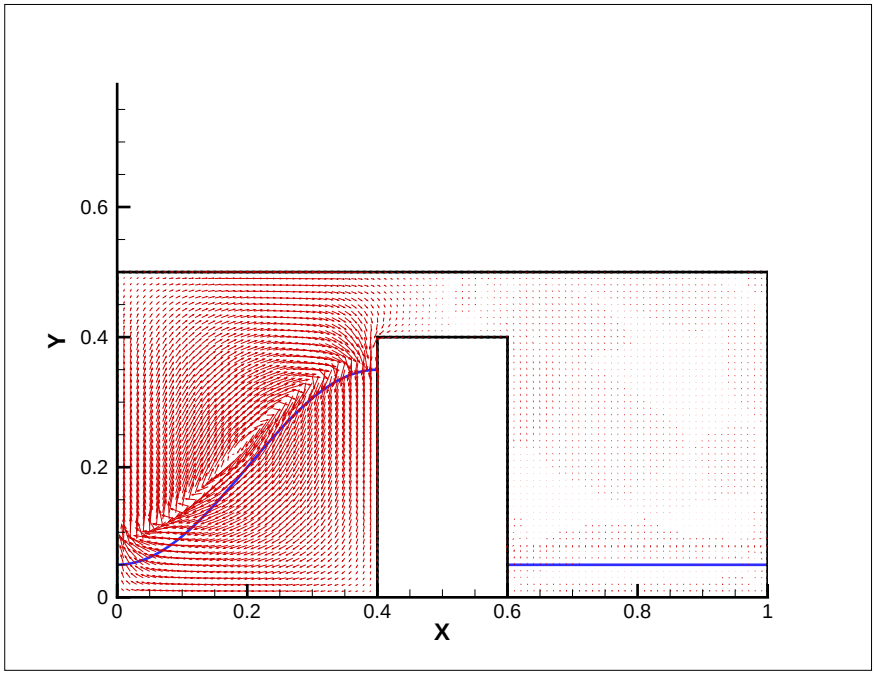

Figure 10: *Initialisation of the test case of the two separated tanks.*

5.2 Water column fall on a dam.

The aim of this second test case is to prove the robustness of the Navier-Stokes equation resolution and the local mass correction algorithm. This test case consists in the computation of a water column fall in a tank. Moreover on the way of the wave at the center of the tank a little rectangular dam has been placed. This test case has been considered by many researchers to validate their models Andrillon *et al.*,[18], Koshizuka *et al.* [19], Ubbink [20] and Greaves [21] among others.

Table 3 details the geometrical, numerical and physical data of the computation. This test case has been simulated on a set of embedded mesh respectively 51×51, 101×101 and 201×201 nodes. The results showing the convergence on the interface position at the different adimensional times $T = t\sqrt{g/a} = 0, 0.809, 1.617, 2.426, 3.233$ nad 4.043 are presented on the figures 13, 14, 15, 16, 17 and 18 in comparison with the experimental pictures tooken by Koshizuka *et al.* [19]. The interface motion is well predicted on the first time step but less then when the interface contorts itself with phenomena of spray and breaking. At $T = 0.809$, the picture shows a spray on the dam, indicating that the water front advancing at the tank bottom already reachs the obstacle. However, the numerical leading edge has not reached yet the obstacle. A $T = 1.617$, the water tongue deflected by the dam is well predicted by the numerical scheme, even if the atomization details of the spray are not resolved . A $T = 2.426$, the water tongue shape is again similar to the experimental one when it moves towards the right wall. A $T = 3.233$, the water came into contact with the right wall and fall under gravity effect. Air has been captured and makes opposition the water fall. The numerical solution is in good agreement with the experiment on this point and the finest mesh 201×201 predicts well the secondary tongue which developps over the dam. A $T = 4.043$, on the meshes

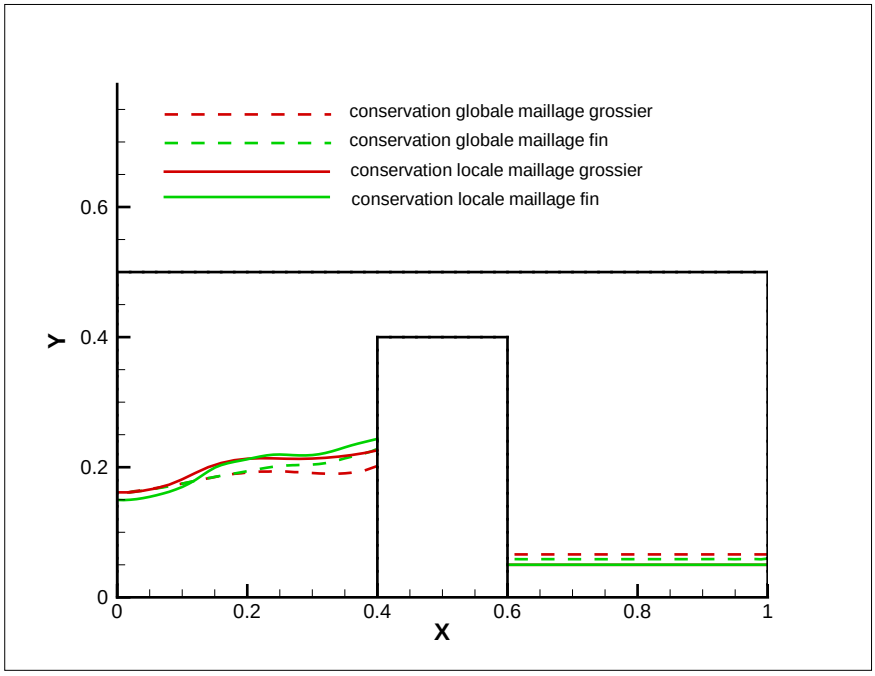

Figure 11: *Interface position at* $t = 1s$. *Mesh convergence and comparison of the two mass correction algorithm.*

101×101 and 201×201 the secondary tongue penetrates in the trapped air phase and dives in the tank bottom.

The simulation showed the ability of the numerical scheme with our mass local corrector to catch the large scale of a breaking wave phenomenum. However, the computation should be refined or adapted in some areas to catch the fine flow details. The computaion, should also be done in three dimensions to catch the surface tension effects which play an important role in the atomization phenomena.

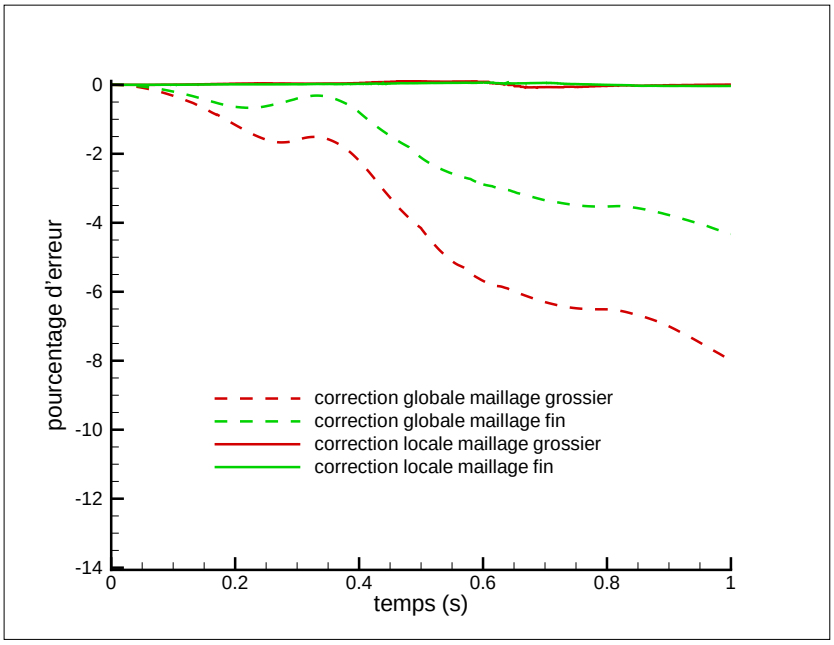

Figure 12: *Evolution of relative error of liquid volume in the left side tank.*

Taille du domaine	:	0.584mx0.584m (maillage $2D$)
Résolution	:	respectivement $4h = 0.01168m$, $2h = 0.00584m$, $h = 0.00292m$
Largeur de la colonne d'eau	:	$a = 0.146m$
Largeur de l'obstacle	:	$L_d = 0.012m$
Hauteur de l'obstacle	:	$h_d = 0.048m$
Abcisse de début de l'obstacle	:	$0.292m$
Tension de surface	:	$\sigma = 0\ N/m$
Densité	:	$\rho_l = 1000\ kg/m^3$ $\rho_g = 1.2\ kg/m^3$
Calcul Euler		
Forces volumiques (gravité)	:	$g = -9.81\ m.s^{-2}$
Epaississement de la Level-Set	:	$\epsilon = 3h$
Pas de temps	:	$\Delta t = 2.10^{-4}s$
pour le maillage grossier		

Table 3: Paramètres pour la simulation numérique du cas test de la chute de la colonne sur une digue.

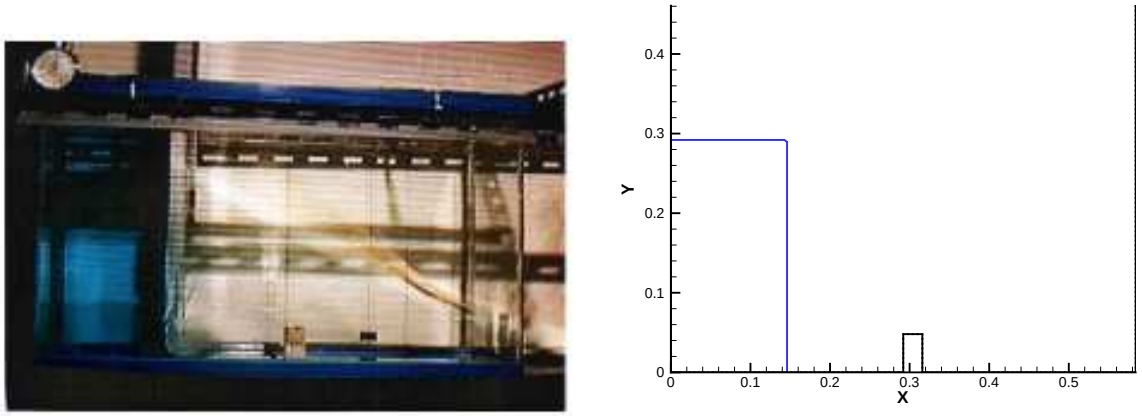

Figure 13: *Initialisation expérimentale [19]. Initialisation de l'interface à* $T = 0+$.

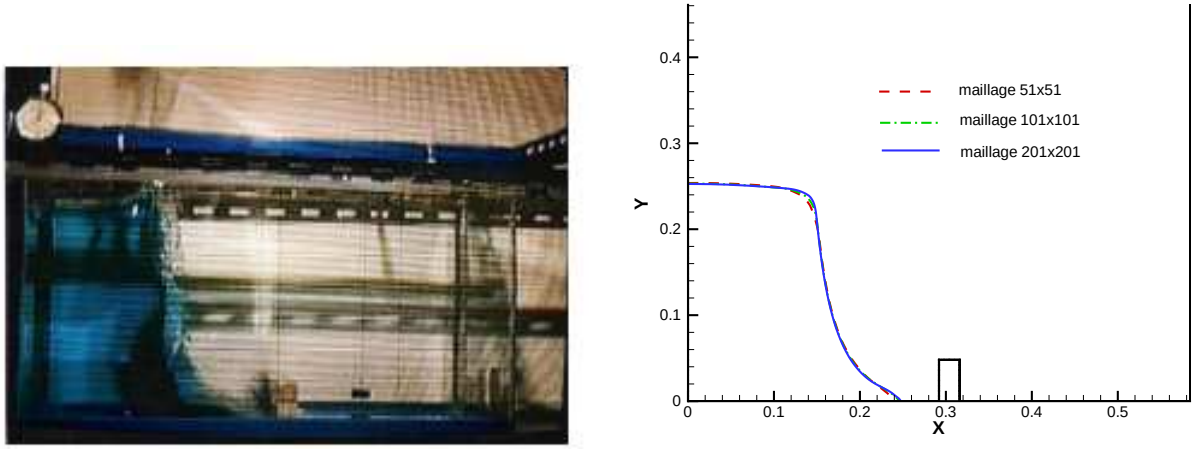

Figure 14: *Comparaison. Visualisation expérimentale [19] et convergence en maillage à* $T = 0.809$.

6 CONCLUSION

In this paper, we have been interested in the mass conservation of each phase for two phase incompressible flow simulation with the Level Set Method. We recall the classic principle of the global mass correction method with the Level Set function. We proposed a discrete conservation law to impose to the discrete characteristic function deduced from the Level Set function. The local corrector stable and accurate. The method extends to any Galerkin discretization. We validated the obtained improvement by comparison of the two algorithm (global and local corrector). The

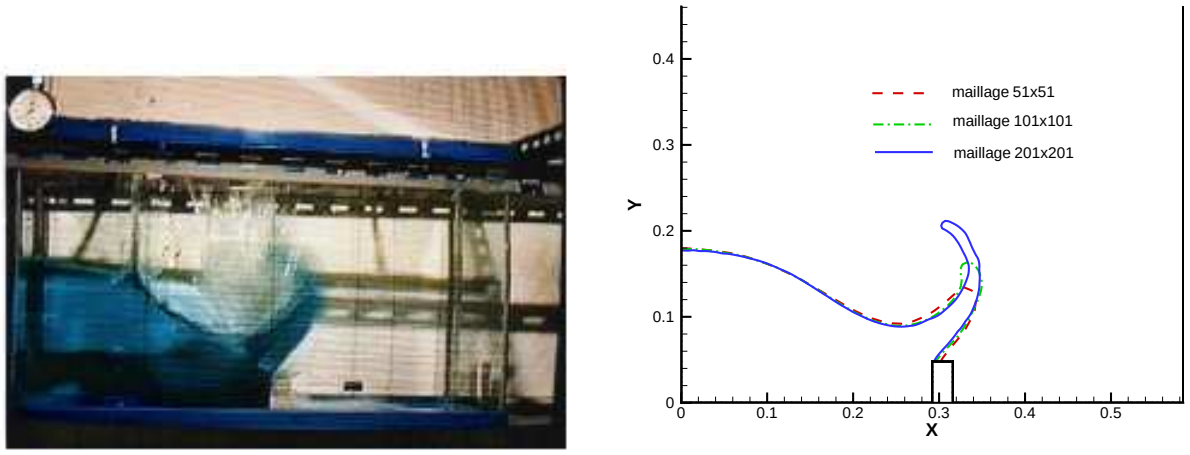

Figure 15: *Comparaison. Visualisation expérimentale [19] et convergence en maillage à* $T = 1.617$.

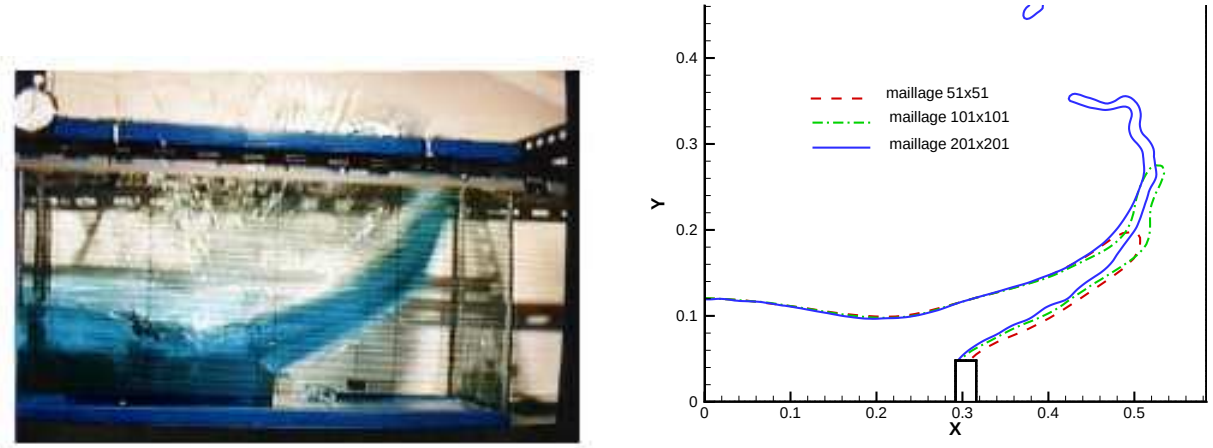

Figure 16: *Comparaison. Visualisation expérimentale [19] et convergence en maillage à* $T = 2.426$.

following step of our work is to integrate the redistanciation in our local corrector. We shall also develop a 3D version of this promising corrector.

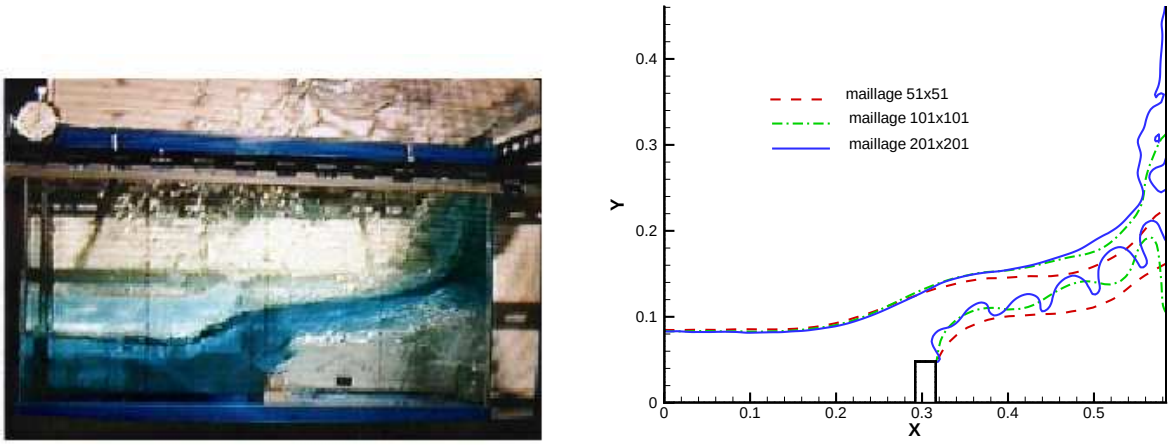

Figure 17: *Comparaison. Visualisation expérimentale [19] et convergence en maillage à* $T = 3.234$.

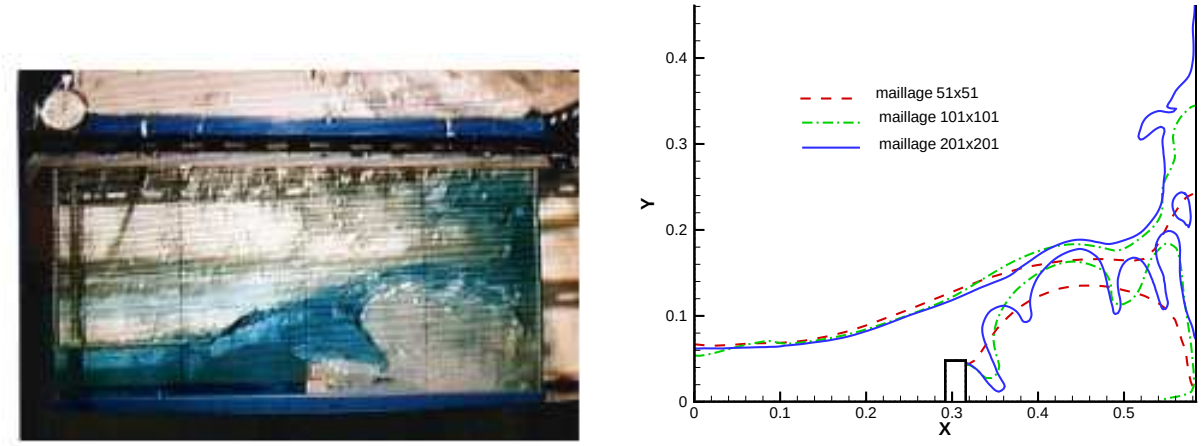

Figure 18: *Comparaison. Visualisation expérimentale [19] et convergence en maillage à* $T = 4.043$.

7 ACKNOWLEDGMENTS

The first author was partly supported by a scientific scholarship of Région Provence-Alpes Côte d'Azur. The third author is supported by a scientific scholarship of CNES.

References

[1] C.W. Hirt and B.D. Nichols, "Volume of Fluid (VOF) methods for the dynamics of free boundaries", *J. Comput. Phys.* **30**, 201-255, 1981.

[2] S. Osher and J.A Sethian. "Front propagating with curvature dependent speed: Algorithms based on Hamilton-Jacobi formulations". *J. Comput. Phys.* **79**:12, 1988.

[3] J.A. Sethian.*Level Set Methods and Fast Marching Methods.* Cambridge University Press, 1999.

[4] S.P. van der Pijl, A. Segal and C. Vuik. "Modeling of three-dimensional bubbly flows with a mass conserving level-set method". *ECCOMAS 2004*, P. Neitaanmaki *et al.* eds. Jyvaskyla, july 24-28, 2004

[5] E. Olsson and G. Kreiss. "A conservative level set method for two phase flow". *J. Comput. Phys.* **210**, 225-246, 2005.

[6] M. Sussman and E.G. Pucket. "A coupled level set and volume-of-fluid method for computing growth and collapse of vapor bubbles". *J. Comput. Phys.* **162**, 301-337, 2000.

[7] A.-C. Lesage, O. Allain, A. Dervieux. "On Level Set modelling of Bi-fluid capillary flow". *International Journal for Numerical Methods in Fluids.* **53**:8, 1297-1314 (2007)

[8] J. Brackbill, D.B. Kothe, C. Zemach. "A continuum method for modeling surface tension", *J. Comput. Phys.* **100**, 335-354, 1992.

[9] R. Löhner, C. Yang and E. Oñate. " Large-scale simulation of flows with violent free surface motion", Proc. of International Conference on Computational Methods in Marine Engineering, MARINE 2005, P. Bergan, J. Gracía, E. Oñate and T. Kvamsdal, Eds, CIMNE, Barcelona, 2005.

[10] S. Osher and J.A Sethian. "Front propagating with curvature dependant speed: Algorithms based on Hamilton-Jacobi formulations", *J. Comput. Phys.* **79**:12, 1988.

[11] J.A. Sethian. "*Level Set Methods and Fast Marching Methods*" . Cambridge University Press, 1999.

[12] S. Osher and R. Fedkiw. "*Level Set Methods and Dynamic Implicit Surfaces*". Springer, 2002.

[13] M. Sussman, E. Fatemi, P. Smereka and S. Osher. "An improved level set method for incompressible two-phase flows." *Computers and Fluids*, **27**(5-6), 663-680 (1998)).

[14] A. Smolianski . Finite-Element/Level-Set/Operator-Splitting (FELSOS) "Approach for Computing Two-Fluid Unsteady Flows with the Free Moving Interfaces". *International Journal for Numerical Methods in Fluids.* **48**:3, 231-269 (2005).

[15] S. Zalesak . Fully multidimensional flux-corrected transport algorithm for fluids. *J. Comput. Phys.* **31**, 335 (1979).

[16] J. Bell, P. Collela, and H.Glaz, A second-order projection method for the incompressible Navier-Stokes equations *J. Comput. Phys.* **85**, 257 (1979).

[17] D. Enright, R. Fedkiw, J. Ferziger, I. Mitchell, A Hybrid Particle Level Set Method for Improved Interface Capturing. *J. Comput. Phys.* **183**, 83-116 (2002).

[18] Andrillon, Y., Alessandrini, B., A 2D+T VOF fully coupled formulation for the calculation of breaking free-surface flow. *Journal of Hydraulic Engineering*, **129:9**, p. 688-696, 2003.

[19] Koshizuka, S., Tamako, H. and Oka, Y., A particle method for incompressible viscous flow with fluid fragmentation. *Computational Fluids Mechanics Journal*, **113**, p. 134-147, 1995.

[20] Ubbink, O., Numerical prediction of two fluid systems with sharp interfaces. *Ph.D. Thesis*, Imperial College of Science, Technology and Medecine, London, 1997.

[21] Greaves, D.M, Simulation of viscous water column collapse using hierarchical grids. *Int. J. Numer. Meth. Fluids* **50**, p.693-711, 2006.

Unité de recherche INRIA Sophia Antipolis
2004, route des Lucioles - BP 93 - 06902 Sophia Antipolis Cedex (France)

Unité de recherche INRIA Futurs : Parc Club Orsay Université - ZAC des Vignes
4, rue Jacques Monod - 91893 ORSAY Cedex (France)
Unité de recherche INRIA Lorraine : LORIA, Technopôle de Nancy-Brabois - Campus scientifique
615, rue du Jardin Botanique - BP 101 - 54602 Villers-lès-Nancy Cedex (France)
Unité de recherche INRIA Rennes : IRISA, Campus universitaire de Beaulieu - 35042 Rennes Cedex (France)
Unité de recherche INRIA Rhône-Alpes : 655, avenue de l'Europe - 38334 Montbonnot Saint-Ismier (France)
Unité de recherche INRIA Rocquencourt : Domaine de Voluceau - Rocquencourt - BP 105 - 78153 Le Chesnay Cedex (France)

Éditeur
INRIA - Domaine de Voluceau - Rocquencourt, BP 105 - 78153 Le Chesnay Cedex (France)
http://www.inria.fr
ISSN 0249-6399